Anat Bashan[1]
Raz Zarivach[1]
Frank Schluenzen[2]
Ilana Agmon[1]
Joerg Harms[2]
Tamar Auerbach[1,3]
David Baram[1]
Rita Berisio[2,*]
Heike Bartels[2]
Harly A. S. Hansen[2]
Paola Fucini[4]
Daniel Wilson[4]
Moshe Peretz[1]
Maggie Kessler[1]
Ada Yonath[1,2]

[1]*Department of Structural Biology, The Weizmann Institute, 76100 Rehovot, Israel*

[2]*Max-Planck-Research Unit for Ribosomal Structure, 22603 Hamburg, Germany*

[3]*FB Biologie, Chemie, Pharmazie, Frei Uni. Berlin, 14195 Berlin, Germany*

[4]*Max-Planck-Institute for Molecular Genetics, 14195 Berlin, Germany*

Received 18 January 2003; accepted 18 February 2003

Ribosomal Crystallography: Peptide Bond Formation and Its Inhibition

Abstract: *Ribosomes, the universal cellular organelles catalyzing the translation of genetic code into proteins, are protein/RNA assemblies, of a molecular weight 2.5 mega Daltons or higher. They are built of two subunits that associate for performing protein biosynthesis. The large subunit creates the peptide bond and provides the path for emerging proteins. The small has key roles in initiating the process and controlling its fidelity.*

Crystallographic studies on complexes of the small and the large eubacterial ribosomal subunits with substrate analogs, antibiotics, and inhibitors confirmed that the ribosomal RNA governs most

Correspondence to: Ada Yonath; email: ada.yonath@weizmann.ac.il

Contract grant sponsor: Max–Planck Society, U.S. National Institute of Health (NIH), the German Ministry for Science and Technology (GMST), and Kimmelman Center for Macromolecular Assembly at the Weizmann Institute

Contract grant number: GM34360 (NIH) and BMBF 05-641EA (GMST)

**Permanent address:* Institute of Biostructure and Bioimage, CNR, 80138 Napoli, Italy

Biopolymers, Vol. 70, 19–41 (2003)

of its activities, and indicated that the main catalytic contribution of the ribosome is the precise positioning and alignment of its substrates, the tRNA molecules.

A symmetry-related region of a significant size, containing about two hundred nucleotides, was revealed in all known structures of the large ribosomal subunit, despite the asymmetric nature of the ribosome. The symmetry rotation axis, identified in the middle of the peptide-bond formation site, coincides with the bond connecting the tRNA double-helical features with its single-stranded 3′ end, which is the moiety carrying the amino acids. This thus implies sovereign movements of tRNA features and suggests that tRNA translocation involves a rotatory motion within the ribosomal active site.

This motion is guided and anchored by ribosomal nucleotides belonging to the active site walls, and results in geometry suitable for peptide-bond formation with no significant rearrangements. The sole geometrical requirement for this proposed mechanism is that the initial P-site tRNA adopts the flipped orientation.

The rotatory motion is the major component of unified machinery for peptide-bond formation, translocation, and nascent protein progression, since its spiral nature ensures the entrance of the nascent peptide into the ribosomal exit tunnel. This tunnel, assumed to be a passive path for the growing chains, was found to be involved dynamically in gating and discrimination. Biopolymers 70: 19–41, 2003

Keywords: *ribosomes; peptide-bond formation; translocation; tunnel gating; elongation arrest*

INTRODUCTION

Over a hundred cellular components are involved the translation of the genetic code into proteins. In rapidly growing cells, the machinery of this fundamental life process constitute about half of the cell's dry weight and consumes up to 80% of the cell's energy. The ribosome, a universal cellular organelle, is the main player in this process, serving as the largest known macromolecular enzyme. All ribosomes are riboprotein assemblies that consist of two subunits of unequal size. The prokaryotic ribosomal small subunit (called 30S) has a molecular weight of 0.85 mega Dalton and contains one RNA chain of over 1500 nucleotides and 20 proteins. The prokaryotic large ribosomal subunit (called 50S) is of molecular weight of 1.5 mega Dalton and contains two RNA chains with a total of about 3000 nucleotides and around 35 proteins. Each of the ribosomal subunits has defined tasks. The smaller ribosomal subunit has key roles in the initiation of the translation process, in choosing the translated frame, in decoding the genetic message, and in controlling the fidelity of codon–anticodon interactions by discriminating against non- and near-cognate amino-acylated tRNA molecules. The larger subunit performs the principal reaction of protein biosynthesis, peptide bond formation, and gates the nascent chains by channeling them through the ribosomal exit tunnel.

Upon initiation of protein synthesis, the two ribosomal subunits associate to form functionally active ribosome. mRNA binds to the small subunit, and amino acids, the building blocks of proteins, are delivered to the ribosome as amino-acylated tRNA molecules. The anticodon loops of the tRNA molecules interact with the small subunit, whereas the acceptor stems bind to the large subunit. Within the ribosome there are three binding sites for tRNA—designated the A (aminoacyl), P (peptidyl), and E (exit) sites—which are partly located on the small and the large subunits. During the elongation cycle both ribosomal subunits work together to translocate all three tRNAs molecules and the associated mRNA chain by precisely one codon, and each of the tRNA molecules passes through the three ribosomal binding sites (A → P→E site). It is conceivable that the translocation of the entire tRNA molecules occurs in a single step, but our findings accord better with the hybrid mode that incorporates intermediate states of uncoupled motions of tRNA features.[1]

We found that correct and precise positioning of the amino-acylated (aa)-tRNA, mandatory for peptide bond formation, is achieved by its remote contacts with the large subunit components. This positioning enables a flip of the 3′ end of the A-site tRNA (to which the amino acid is bound) into the site of the 3′ end of the P-site tRNA, in concert with peptide bond formation. This A→P flipping motion has a spiral nature, which directs the newly created peptidyl into the exit tunnel and enables the movement of the deacylated P-site tRNA into the E site.[2,3] Below we show that once the amino-acylated tRNA is placed properly, by utilizing internal ribosomal symmetry, a mutual orientation enabling peptide bond formation, is reached. We also show that the ribosomal exit tunnel possesses capabilities for sequence discrimination and elongation arrest.

THE EARLY DAYS OF RIBOSOMALCRYSTALLOGRAPHY

Ribosomal crystallography, initialized by us over two decade ago,[4] yielded recently high-resolution crystal structures of free or complexed ribosomal particles, emerging in an impressive speed and leading to a quantum jump in the understanding of the translation process. We first established that the key to obtaining ribosomal crystal is to use highly active homogenous preparations under conditions similar to their in situ environments. Ribosomes from robust organisms were chosen assuming that they would maintain their integrity during preparation, hence should provide suitable material for crystallization. We further minimized crystal heterogeneity by inducing selected conformations within the crystals. We also designed complexes containing ribosomes at defined functional stages, such as of the entire ribosome with tRNA and mRNA molecules.[5] This approach was later adopted, refined and extended, and has led a medium resolution structure of the ribosome with three tRNA molecules.[6]

The first crystals that yielded some crystallographic information were grown from of the large subunit from *Bacillus stearothermophilus.*[4,7] Crystals of the large and the small subunits from *Thermus thermophilus,* T50S[8,9] and T30S,[10] diffracting to low resolution, were grown later. At approximately the same time, a Russian group, headed by A. Spirin and B. Weinstein, obtained microcrystals of the latter.[11] In parallel, we initiated crystallographic studies on ribosomes from *Haloarcula marismortui,* an archaeon residing in the Dead Sea, the lake of the highest salinity in the world. It took a few years to progress, step by step, from microcrystals[12] of the large ribosomal subunit from *H. marismortui,* H50S, via crystals diffracting to medium resolution,[13] towards high-resolution diffraction.[14]

The recent addition of *Deinococcus radiodurans,* an extremely robust Gram-positive mesophilic eubacterium that shares extensive similarity with *Escherichia coli* and *T. thermophilus,* proved to be highly successful. Thus, crystals of the large ribosomal subunit from *D. radiodurans,* D50S, and of their complexes with antibiotics and substrate analogs could be grown and kept under conditions almost identical to those optimized for maximizing their biological activity[15,16] These crystals were found to provide an excellent system to investigate the peptide-bond formation[2]; to gain more insight into functional flexibility[16,17]; to reveal the structural basis for antibiotics binding and resistance, thus providing tools towards structural based drug design[18,19]; to identify the exit tunnel discriminative gate and to reveal the structural basis for the involvement of the ribosome in cellular regulation.[3,20]

Deinococcus radiodurans was originally identified as a contaminant of irradiated canned meat, and later isolated from environments that are either very rich or extremely poor in organic nutrients, ranging from soil and animal feces to weathered granite in a dry Antarctic valley or room dust. It is the organism with the highest level of radiation resistance currently known, and can live in wastes of atomic piles and irradiated medical instruments. It survives under conditions that cause DNA damage, such as hydrogen peroxide, and ionizing or uv radiation. It contains systems for DNA repair, DNA damage export, desiccation, starvation recovery and genetic redundancy,[21] and its genomic material is tightly packed.[22]

All ribosomal crystals were found to present challenging technical problems, owing to their enormous size, their complexity, their natural tendency to deteriorate and disintegrate, their internal flexibility, and their extreme sensitivity to irradiation. Assuming that one of the main reasons for crystal decay is the progression of free radicals that are produced by the x-ray beam, we pioneered crystallographic data collection at cryogenic temperature.[23,24] This procedure minimizes dramatically the harm caused by irradiation, and therefore became rapidly the routine way for collecting crystallographic data from biological crystals. The application of cryo crystallography alongside advances in the methodology of x-ray crystallography, including the installation of third generation synchrotrons equipped with state-of-the-art detectors, and the increased sophistication in phasing procedures, enabled us, as well as others, to handle most of the technical problems of the ribosomal crystals.

ON THE ARCHITECTURE OF THE RIBOSOME

The interface views of the small and the large eubacterial ribosomal subunits are shown in Figure 1. In both subunits the ribosomal RNA dominates most of the ribosome structure and each of them utilizes its flat face for intersubunit interactions. Docking of the mRNA and tRNA onto the structures of the ribosomal particles determined by us, using the 5.5 Å structures of the complex of the entire ribosome with three tRNA molecules[6] revealed the regions that contact the tRNA molecules in both subunits (Figure 1) and reconfirmed that the anticodon loops of the A- and P-site tRNAs as well as the mRNA do not contact any ribosomal proteins.

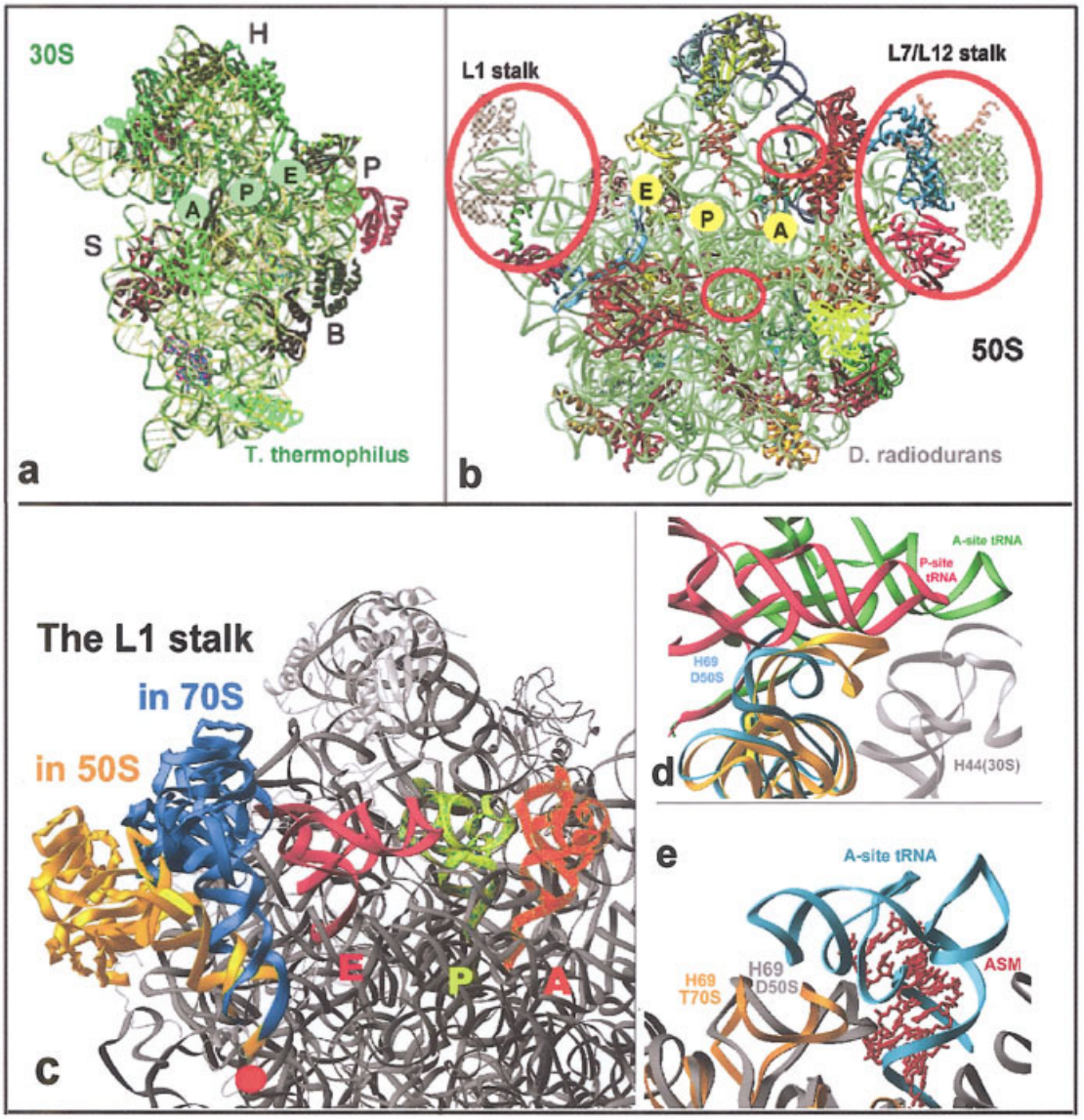

FIGURE 1 The upper panel (a) and (b): The "front views" (the subunit interfaces) of the two eubacterial ribosomal subunits, as determined by us.[15,28] The backbone of the ribosomal RNA is shown in light green. The proteins are colored arbitrarily. The ribosomal features related to the text are depicted and colored. The main structural features are indicated. H, S, P, and B designate the head, shoulder, platform, and body of the small subunit. A, P, and E designate the three tRNA molecules. Their interactions sites with the small subunit (namely, the approximate positions of the anticodon loops) and the large subunit are shown in green and yellow, respectively. The red rings indicate some of the regions that are disordered in H50S.[32] (c) The top-left (L1 stalk) and (d) the middle (H69) encircled regions are highlighted in the lower panel. (c) Zoom into the left upper part of the large subunit front view. The positions of the L1 stalk in the assembled T70S ribosome (in blue) and in the unbound D50S large subunit (in gold). The pivot point is marked by a red dot. A-P-, and E tRNA were docked from the structure of T70S.[6] The backbone of the ribosomal RNA and the ribosomal proteins are shown in gray. (d) Hints at a possible mechanism for the creation of the intersubunit bridge B2a (H69). The structures of H69 in the assembled ribosome (in gold) and in the unbound large subunit (cyan) is shown in relation to the components of the initiation complex, represented by H44 of the small subunit (gray), the initiator P-site tRNA (pink), and the A-site tRNA (green). (e) The orientation of the A-site tRNA (cyan) and its mimic, called ASM[2] (in red) in relation to the two conformations of H69, hinting at the possible dynamic role of H69 in translocation.

Common to both subunits are the overall structures of the ribosomal proteins and their distribution. Almost all ribosomal proteins contain long tails or extended internal loops. In general, the globular domains are peripheral, located on the particle's surface, at its solvent side. The involvement of proteins in the stabilization of the structure is achieved mainly through their long extensions that penetrate into rRNA regions and serve as molecular linkers, struts and supports, as observed in viruses.[25] Another group of proteins have tails pointing towards the solution, similar to their positioning in the nucleosome,[26] presumably acting as tentacles that enhance the binding of non-ribosomal compounds that interact with the ribosome.[17,27] A few proteins are built of globular domains and do not have extensions. These are located either at the ends of functionally important protuberances or fill-up gaps between features. One of them, CTC, which in *D. radiodurans* is built of three domains, two of which may play a role in survival mechanisms, is described below and in Ref. 15.

The global organizations of the two subunits are rather different. Whereas the small one is built of well-defined structural domains, each related to the two-dimensional organization of the ribosomal RNA, the core of the large subunit seems to be more compact. Despite this compact appearance, the striking architecture of the large subunit allows for substantial domain mobility, while maintaining relative rigidity of local structural features. Long extensions and loops of ribosomal proteins as well as specific RNA folds are stabilizing these features, by several means, such as A-minor packing and high G–C content at the rims of strategically located junctions.

Two groups, ours[28] and that of V. Ramakrishnan, MRC, UK,[29] determined independently the high-resolution structure of the small subunit from *T. thermophilus* (T30S). Although different phasing procedures were employed, the resulting structures are very similar. Both contain the morphological features familiar from early electron microscopy studies.[30,31] Both show that the main structural features of this subunit—a "head," a "neck," and a "body" that contains a "shoulder" and a "platform" (Figure 1), radiate from the junction combining the head and the body, a location that also hosts the decoding center.

The head and the shoulder play a key role in mRNA binding, as they form the elongated, curved channel, which we assigned as the path of the mRNA chain.[28] A latch, which can be described as a noncovalent body–head connection is formed by the shoulder and the lower part of the head, is the feature that forms the entrance to the mRNA channel. This latch facilitates mRNA threading, and provides the special geometry that guarantees processivity and ensures maximized fidelity. It controls the entrance to the mRNA channel by creating a pore of varying diameter and its relative location is dictated by the head twist. The decoding region contains features from the upper part of the body and the lower part of the head. Mapping the conserved nucleotides on our structure showed remarkable conservation around this region, in accord with the universality of the decoding process.

The availability of two high-resolution crystal structures of unbound large ribosomal subunits, from archaea, H50S[32] and eubacteria D50S,[15] as well as a lower resolution structure of the large subunit within the assembled eubacterial ribosome,[6] provides a unique tool for comparative studies. The common view of the large subunit, as obtained by electron microscopy,[33,34] often called the "crown view," looks like a halved pear with two lateral protuberances, called the L1 and L7/L12 stalks. Although different in the inclination of the protuberances, the shapes of the unbound large subunit within the assembled ribosome, as well as the unbound D50S (Figure 1), are similar to this traditional view. The structure of H50S, however, lacks both lateral protuberances because they are disordered, as in the case for almost all functionally relevant features of H50S.[32] It is likely that these striking differences are correlated with the conditions under which the two structures have been determined. Whereas D50S crystals were grown and maintained under conditions almost identical to those determined for optimized functional activity,[15] the H50S crystals contain solvent of composition far from their in situ environment.[35] Thus, whereas *H. marismortui* contain over 3*M* KCl, the crystals of H50S contain only about 1.5*M* NaCl,[32] conditions that allow a very low level of protein biosynthesis.[12]

Peptide-bond formation, the principal reaction of protein biosynthesis, has been localized within a conserved region in the large subunit over three decades ago, and later was shown to consist solely on RNA.[36–40] The peptidyl transferase center (PTC) is situated above the entrance to the polypeptide exit tunnel, a major component of the ribosome that could be detected even by conventional electron microscopy at low resolution.[41,42] Despite their low resolution, these studies showed that this tunnel spans the large subunit from the location assumed to be the peptidyl transferase site to its lower part, consistent with a suggestion that the newest synthesized part of a nascent protein is masked by the ribosome.[43,44]

Among the 43 nucleotides forming the active site, namely the PTC,[36] are conserved in *H. marismortui* and *D. radiodurans.* Superposition of the PTC of

H50S and of D50S on the corresponding region within T70S, shows similar, albeit not identical, folds. The orientations of some of the nucleotides, however, show distinct differences.[6,15] It is conceivable that the different orientations reflect the flexibility needed for the formation of the peptide bond. It is also possible, however, that the different orientations result from the differences in the functional states of the 50S subunit in the two crystal forms, consistent with the structural changes of distinct nucleotides of the peptidyl transferase ring that occur upon transition between the active and inactive conformations.[45]

The comparison between H50S and D50S shed light also on the correlation between structure, function, environment and phylogenetic aspects. For example, some D50S ribosomal proteins show remarkable differences, even when sharing homology with their counterparts in H50S. Others share structural features, with no or little sequence homology.[46] In addition, D50S contains several proteins that have no counterparts in H50S, and we detected RNA segments replacing proteins and vice versa. Of structural interest is a three-domain protein (CTC), an extended α-helical protein (L20) and two Zn-finger proteins, L32 and L36.[15]

ANTIBIOTICS: STICKS IN THE WHEELS OF THE TRANSLATION MACHINERY

Antibiotics are natural or human-made compounds, designed to interfere with bacterial metabolism or eliminate bacteria by inhibiting fundamental cell processes such as the biosynthesis of proteins or DNA or cell wall components. As a central element of the cell cycle, the ribosome is one of the main targets for a broad range of antibiotics. Indeed, about 40% of the known antibiotics interfere with protein biosynthesis.[47–51] These include structurally diverse natural and synthetic compounds that efficiently inhibit the ribosomes function. Theoretically, the ribosome offers multiple opportunities for the binding of small compounds, but practically all the known drugs utilize only a few sites. Biochemical information about binding and action of antibiotics on the ribosome has been accumulated for almost four decades, but exact biding information had to await the determination of the ribosome structure. Analysis of the antibiotics binding modes was found to assist not only the understanding of the drug action, but also shed light on problems associated with medical treatment. Among those is the superior ability of bacteria to rapidly acquire antibiotic resistances, which became a major handicap in modern medicine.

The binding modes of over a dozen antibiotics that target the ribosome have been determined crystallographically at relatively high resolution.[3,18–20,27,52–54] The two crystallizable ribosomal subunits from eubacteria, T30S[28,29] and D50S,[15] were found suitable to serve as pathogen models, since they bind quantitatively clinically relevant antibiotics using concentrations comparable to those used in medicine in fashion similar to that of the pathogen. We could localize unambiguously the antibiotic drugs in crystals of their complexes with the ribosomal subunits. Preferably, co-crystals were grown. Alternatively, crystals of ribosomal particles were soaked in solutions containing the antibiotics. In several cases the co-crystals yielded crystallographic data of higher quality than the crystals of the free particles, presumably because the binding of the antibiotics limited internal motions of flexible regions, thus increasing the homogeneity.

Most of the antibiotics studied by us were found to bind primarily to ribosomal RNA and did not cause major conformational changes.[18–20,27,51] However, a few trigger significant allosteric alterations.[2,27,51] Analysis of the structures of the antibiotics complexes indicated a high diversity in their modes of action. In general, they either interfere with substrate binding or hinder the mobility required for the biosynthetic process or block the tunnel that provides the path of the nascent proteins.

Antibiotics Targeting the Small Subunit

Aminoglycosides are known to render the translational apparatus highly inaccurate. They bind adjacent to the decoding site and influence its orientation. Paromomycin, for example, induces a conformational change that enhances the affinity of near-cognate tRNAs to the A site. Hygromycin B and neomycin restrict the necessary movements of the decoding region, thus freezing the tRNA in the A site.[52,53]

Tetracycline is a broad-spectrum antibiotic that was found to bind to multiple positions in the ribosome. Among its six binding sites to the small ribosomal subunit (Figure 2), a single site is responsible for their physiological inhibitory action, namely the blockage of the A site.[27,52] Consistently, this binding site is in close proximity to the 23S RNA mutations that acquire tetracycline resistance.

The formation of the initiation complex, involve the small subunit, mRNA, initiator tRNA (in bacteria fMet–tRNA^{fMet}), and three initiation factors (IF1, IF2, and IF3). This step is inhibited by edeine (Figure 2) and pactamycin, two universal antibiotics that cause displacement of the mRNA.[27,52] Edeine also induces an allosteric base pair between the major helices of

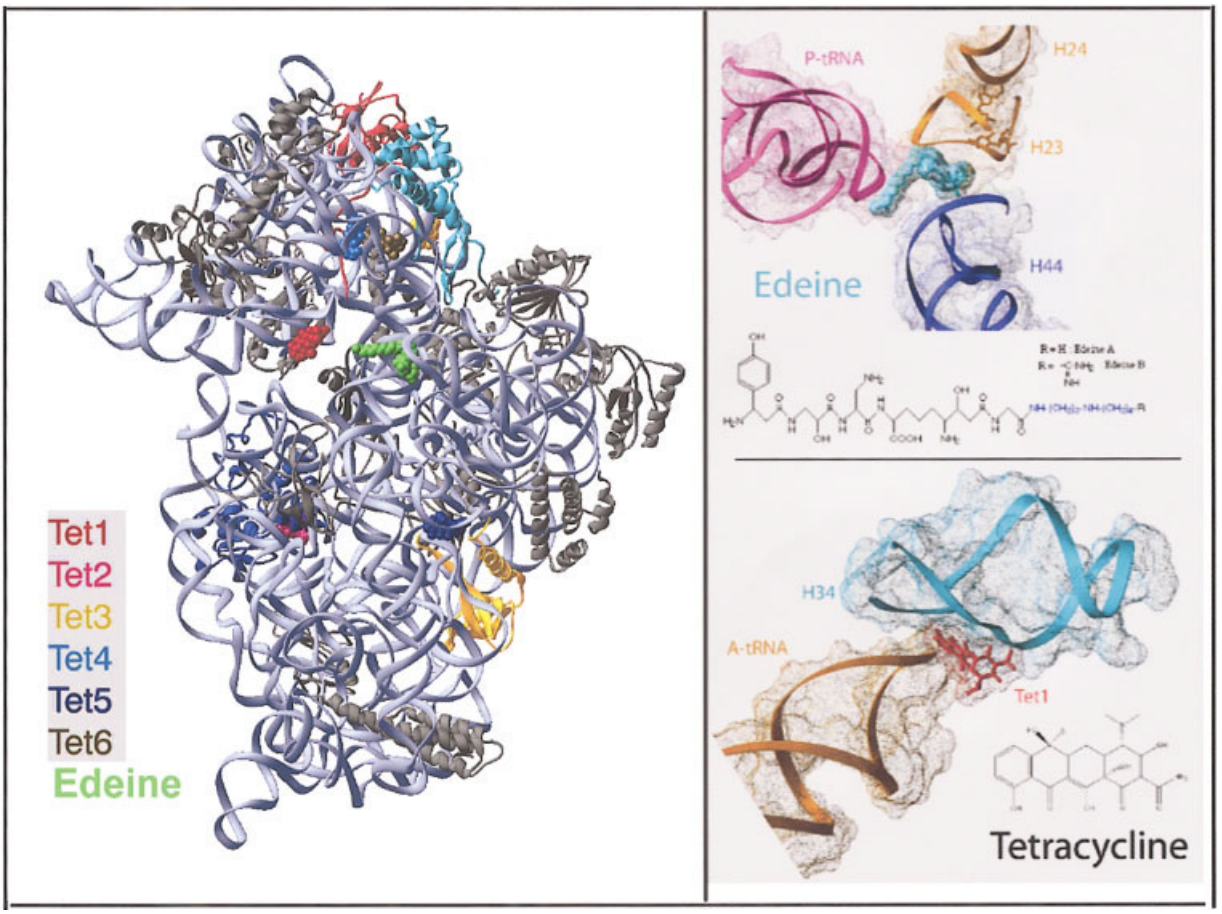

FIGURE 2 Left: The locations of edeine and the six different binding sites of tetracycline in the small subunit. Right: Space filling representations of the physiologically relevant binding sites of edeine and tetracycline, with their chemical formulas.

the platform, thus limiting its conformational mobility (for more detail see below, in the section Limited Platform Mobility Stalls Protein Biosynthesis), influencing the positioning of P-site tRNA and hampering the regulatory action of IF3.[27] Spectinomycin is an additional antibiotic agent that acts by limiting the ribosomal mobility. It was shown to trap the head at a particular conformation, thus hindering motions necessary for translocation.[53]

Antibiotics Targeting the Large Subunit

Many clinically useful antibiotics target the large subunit in the PTC, its vicinity or at the entrance to the ribosome tunnel (Figure 3). Chloramphenicol binds to the PTC and interferes with A-site binding since it occupies the position of the amino acid attached to the A-site tRNA. The lincosamides (e.g., clindamycin and lincomycin) interact with both the A and P site on the 50S ribosomal subunit, thus preventing peptide-bond formation.[18]

Puromycin and sparsomycin are universal inhibitors of protein biosynthesis that exerts their effect by direct interactions with the PTC. Because of their absolute universality, they serve as tools for investigating the mechanism of peptide-bond formation, rather than used as clinically relevant antibiotic agents.[38,39,55–59] Puromycin resembles the 3′-terminus of aminoacyl–tRNA, but its aminoacyl residue is linked via a nonhydrolyzable amide bridge instead of an ester bond. Sparsomycin is less useful as a substrate mimic since it binds to the center of the PTC and triggers significant conformational alterations in both the A and the P sites.[2] Although, consistent with biochemical findings,[60] it forms only a few stacking interactions with one ribosomal nucleotide, A2602, due to the mobility of this nucleotide it influences the positioning of both tRNA molecules and may enhance nonproductive tRNA binding. This explains its interference with the binding of A-site antibiotics, like chloramphenicol, and the increased tolerance to sparsomycin of strains with mutations of A-site nucleotides.[61,62]

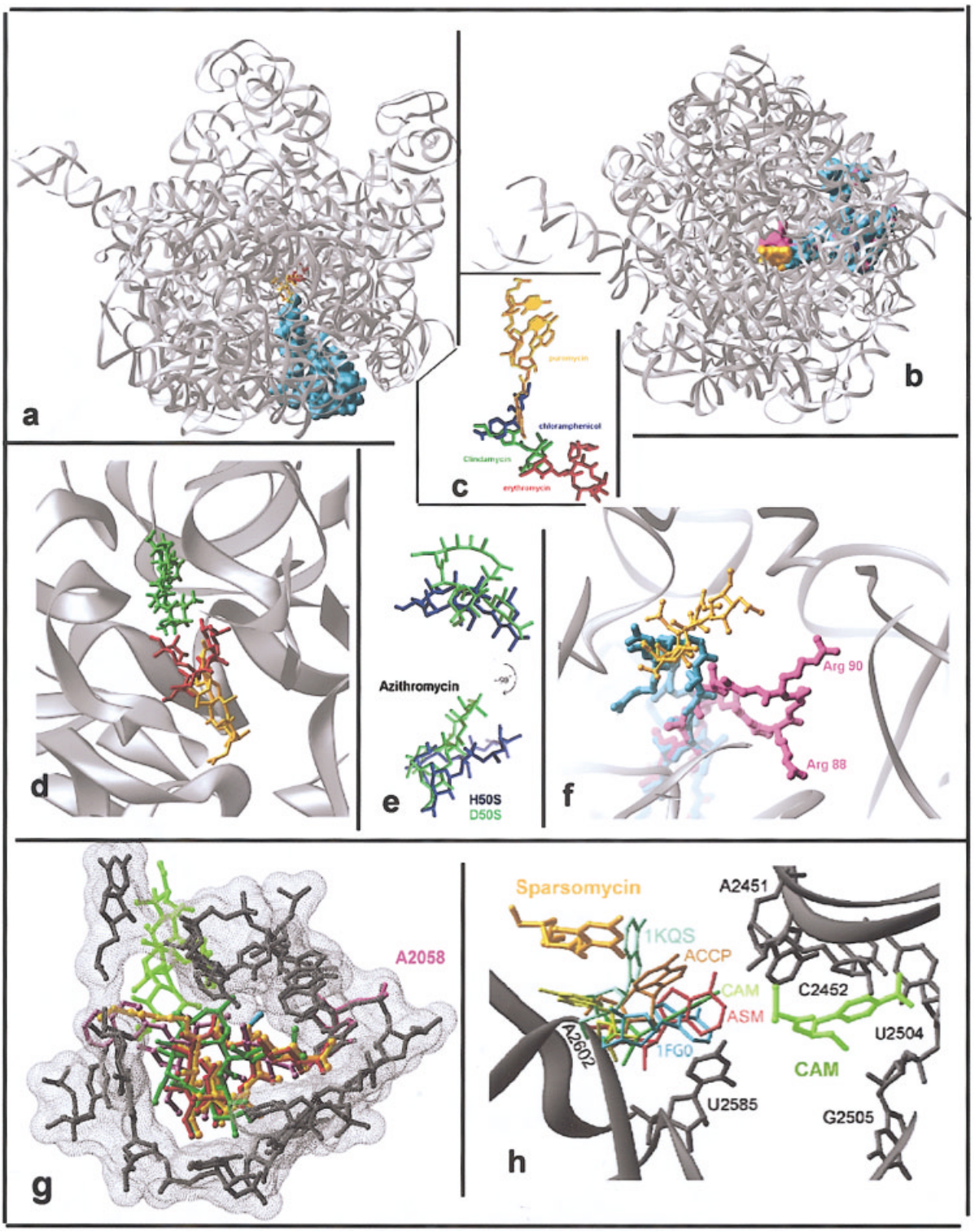

FIGURE 3

Among the antibiotics that target ribosomes, macrolides rank the highest in clinical usage. Most macrolides have a broad-spectrum antimicrobial activity and are used primarily for respiratory, skin, and soft tissue infections. The macrolide family is large and structurally diverse, but all share a central lactone ring of 12–16 members. All macrolides studied so far bind at the entrance of the ribosomal exit tunnel (Figure 3).

However, their binding modes, their exact positions, and their precise inhibitory mechanisms may vary significantly.[3,18–20,54]

The binding site of 14-membered macrolides is somewhat distant from the PTC, so that a polypeptide chain of 5–6 amino acids can be produced before the elongation is stalled. A2058 is the key determinant for their binding. It interacts with the macrolides via their desosamine sugar.[18,19] Human-made improved antibiotics (e.g., acid-stable and broader spectrum), i.e., chlarithromycin or roxithromycin,[18] bind in a similar way. The observed interactions of the macrolides with D50S are consistent with drug resistance in clinical pathogens caused by the substitution of A←G or by the methylation of A2058. Similarly, G in 2058 position acquires selectivity to 14-member macrolides between prokaryotes and eukaryotes.[48,50] In this respect *H. marismortui,* being an archae, resembles eukaryotes rather than eubacteria, since its corresponding base is a guanine.

The 15 and 16 members macrolides are less selective, and by the use of extremely high concentrations of the antibiotic agents, namely in the milimolar range,[54] compared to the clinically used micromolar amounts, compounds such as carbomycin A and josamycin could be bound to H50S. These compounds posses long extensions of the desosamine sugar, which, in H50S complexes, make extensive contacts with the environment of the P site,[54] presumably to compensate for the lost interactions with A2058. Indeed, a noticeable difference in the positioning and orientation could be detected between the modes of binding of antibiotics to the eubacterial D50S[19] and the archael H50S,[54] even for azithromycin, a 15-member macrolides with no large extensions.

Two recently developed macrolide derivatives are the ketolides and the azalides, which provide major improvements of the pharmacokinetics and enhanced activity against certain macrolide-resistant pathogens. The binding modes of the azalide azithromycin and the ketolide ABT773 to D50S explain their improved properties. Thus, azithromycin was shown to bind cooperatively to two sites within the exit tunnel (Figure 3); and ABT773 binds to a larger portion of the large subunit, reaching from domain V, the site of the PTC towards domain II of the 23S RNA and linking RNA features that are positioned at a large sequence distance.[19]

The most striking binding mode has so far been observed for troleandomycin (TAO), a semisynthetic derivative of erythromycin, in which an oxirane ring replaces a methyl of the lactone and all moieties capable of participating in hydrogen bonding have been either methylated or acetylated.[63] As found for other macrolides, azalides, and ketolides,[18,19,54] TAO binds to the large ribosomal subunit close to the tunnel entrance, and although all the commonly observed interactions of the macrolides cannot be formed by this compound, it binds to eubacterial ribosomes exploiting the macrolide favorable binding site, the vicinity of A2058. However, the orientation of TAO within the tunnel is rather unique (Figure 3),

FIGURE 3 *In all:* D50S RNA is represented by gray ribbons. (a) and (b) show the location of the entrance to the protein exit tunnel, just below the PTC. Views along (a) and into (b) the tunnel from the PTC are shown. Protein L22 is shown as a space-filled model, either in cyan (the native conformation) or magenta (the swung conformation), within the backbone of D50S RNA. Erythromycin [(in (a)] is shown in red and TAO (in (a) and in (b) in gold. (c) The overlapping binding sites of puromycin (in yellow), representing the approximate position of the CCA end of A-site tRNA) and chloramphenicol (blue), clindamycin (green), and erythromycin (red). (d) The location of macrolides within the exit tunnel. A five-residue peptide is shown in gray. Its upper end designates the position of the PTC. Erythromycin is shown in red, and TAO in gold. The direction of the tunnel is approximately vertical, with its opening at the bottom, about 90 Å below TAO's the lowest part. (e) Superposition of the binding sites of azithromycin the archael H50S[54] (in blue) and in the eubacterial D50S[19] (in green). (f) The positions of the two conformations of the tip of the β-hairpin of protein L22 within the tunnel. The native conformation is shown in cyan, and the swung conformation in magenta. TAO is gold. (g) The binding modes of several antibiotics within a cross section of the entrance to the tunnel in D50S. The binding nucleotides are marked. The position of the key nucleotide for selectivity and resistance, A2058 is marked by pink. Red: erythromycin; cyan: claritromycin; gold: roxythromycin; light green ABT-773; green and dark-pink are two molecules of azythromycin. (h) The positions of chloramphenicol (CAM) and sparsomycin in the PTC. The dark gray indicates the RNA backbone in the sparsomycin/D50S complex. The light gray shows the backbone in the D50S/CAM complex. The different orientations of A2602 in complexes of H50S and D50S with several substrate analogs, chloramphenicol, and sparsomycin are shown (identified by their names or their Protein Data Bank entries).

presumably dictated by its size and chemical properties. Thus, it is located somewhat deeper in the tunnel and instead of being nearly perpendicular to the tunnel wall, its lactone ring is almost parallel to it. Furthermore, in contrast to erythromycin and its family that interact exclusively with domain V of the 23S RNA, TAO interacts also with domain II (helices H35 and H35a), consistent with the cross-resistance between TAO and ABT-773 mutants, induced by us in *D. radiodurans,* and with the interactions of the latter with domain II.[3,19,20]

In addition, TAO interacts with protein L32, and hits a specific element of the tunnel wall—namely, the tip of protein L22 β-hairpin.[20] Consequent significant conformational alterations in the exit tunnel are caused, since one of these arginines is embedded in a narrow groove that should limit the space available for its conformational rearrangements, causing a swing of the entire tip across the tunnel (Figure 3). The tip of L22 β-hairpin consists of 11 residues, and contains a short loop made of a highly conserved arginine, an invariant alanine and a residue, which in most species is either an arginine or a lysine (residues 88–90). This short loop seems to act as a double hook for interacting with the tunnel wall. Thus, in the native as well as in the swung conformations this short loop makes extensive interactions with the tunnel walls, so that both conformations are stabilized mainly by electrostatic interactions and hydrogen bonds with the backbone of rRNA. A pronounced positive surface charges[65] of the region adjacent to the L22 hinge area seems to facilitate the precise positioning of L22 hairpin stem, required for enabling the accurate swing motion and the anchoring of the double hook to both sides of the tunnel.

CORELATED MOBILITY, FLEXIBILITY, AND FUNCTIONAL ACTIVITY

The ribosome is a precisely engineered molecular machine that performs an intricate multistep process that requires smooth and rapid switches between different conformations. Hence, all major events involved in protein biosynthesis require significant mobility. Analysis of the high resolution structures of the ribosomal particles combined with comparative studies indicated that both ribosomal subunits contain structural elements capable of global motions and local rearrangements, and undergo reversible alterations during the process of protein biosynthesis. Some examples are given below.

Conformational Mobility Facilitating mRNA Threading and Progression

Conformational variability of the small subunit was detected by various methods, including cryoelectron microscopy,[66,67] and head mobility was confirmed by molecular replacement studies using the low-resolution crystals.[17,28] Analysis of the high-resolution structure of T30S Figure 1a suggested an interconnected network of features allowing concerted motions during translocation, assisting the correct mRNA threading and progression by providing the geometry required to guarantee processivity and to ensure maximized fidelity. These motions include the formation of a pore of varying size between the head and the shoulder, in conjunction with the displacement of the platform. The pivotal point for this motion is likely to be at the connection between the head and the neck of the small subunit, near the binding site of the antibiotic spectinomycin, which hampers the head twist by trapping a particular conformation.[53]

Because of its significant conformational flexibility, the small ribosomal subunit is less stable than the large one. We found that by exposing 70S ribosomes to a potent proteolytic mixture, the 50S subunits remained almost completely intact, whereas the 30S subunits were severely damaged. Similarly, large differences in the integrity of the two subunits were observed when attempting crystallization of entire ribosomes assembled from purified subunits. Crystals obtained from these preparations were found to consist only of 50S subunits[68,69] and the supernatant of the crystallization drop contained only fragmented 16S RNA chain and the 30S ribosomal proteins. Consequently, among the many ribosome sources that were tested, so far only the 30S from *T. thermophilus* crystallized, and only one crystal type of the small subunit was found suitable for crystallographic studies. Almost a decade was needed to minimize the severe nonisomorphism of this form and all the procedures developed for increasing the homogeneity of these crystals are based on postcrystallization treatments.

We induced preferred conformation within the T30S crystals by exposing the T30S crystals to elevated temperatures, exploiting the commonly used heat-activation procedure.[70] Once functional activation was achieved, the conformation of the particles was stabilized by incubation the crystals with minute amounts of a heteropolytungstate cluster of 18 tungsten atoms.[71] Postcrystallization conformational rearrangements resulted in a conformation resembling that suitable for initiation. The stabilization of the head, one of the most dynamic features, was achieved

by the interactions of four W18 clusters with protein S2. This large and flexible ribosomal protein is located on the solvent side of the 30S particle and interacts with both the head and the body. Since in T30S crystals, protein S2 is located in the proximity of the crystallographic twofold axis, the S2 proteins of two 30S subunits interacted via a total of eight W18 clusters. These "glued" the symmetry-related two particles hindered the motions of protein S2 and consequently of the head.

The W18 cluster played a dual role in the course of structure determination of T30S. In addition to minimizing the conformational heterogeneity and limiting the mobility of the crystallized particles, treatment with this cluster yielded phase information. Thirteen W18 clusters bind to each T30S particle. The individual W atoms of ten of them (total 180 atoms) could be located precisely. Most of tungsten clusters were found to interact with ribosomal proteins, in positions that may significantly reduce the global mobility of the T30S particles within the crystal network. Pairing of T30S particles around the crystallographic twofold axis is one of the main features of the crystallographic network in T30S crystals. The contacts holding these pairs are extremely stable, and many of them were maintained even after the rest of the crystal network is destroyed.[72]

Limited Platform Mobility Stalls Protein Biosynthesis

The small subunit is the main player in initiation of protein biosynthesis. After binding to the mRNA the initiation complex moves in the 5′ to 3′ direction along the mRNA scanning it, in search for the initiator (AUG) codon.[73] Edeine is a peptide-like antibiotic agent, produced by a strain of *Bacillus brevis*. It contains a spermidine-type moiety at its C-terminal end and a β-tyrosine residue at its N-terminal end.[74] As early as 1976[75] it was found that the universal antibiotic edeine blocks mRNA binding to the small ribosomal subunit.

We found that it binds to the platform in a position that may influence the binding of the P-site tRNA, alter the mRNA path at the E-site, and hamper the interactions between the small and the large subunits.[27] This is consistent with the finding that a subset of the 16S rRNA nucleotides protected by the P-site tRNA[76] overlaps with those protected by edeine, kasugamycin, and pactamycin.[77,78] In addition, the binding of edeine to the 30S subunit induces the formation of a new base pair[27] that may alter the mRNA path and would impose constraints on the mobility of the platform. Thus, by physically linking the mRNA and four key helices that are critical for tRNA and mRNA binding, edeine locks the small subunit into a fixed configuration and hinder the conformational changes that accompany the initiation process.

The universal effect of edeine on initiation implies that the main structural elements important for the initiation process are conserved in all kingdoms. Analysis of our results shows that all rRNA bases defining the edeine-binding site are conserved in chloroplasts, mitochondria, and the three phylogenetic domains. Among these are two conserved nucleotides along the path of the messenger. Thus, edeine shows a novel mode of action, based on limiting the ribosomal mobility and/or preventing the ribosome from adopting conformations required for its function. Furthermore, it induces an allosteric change by the formation of a new base pair—an important new principle of antibiotic action.

E-Site tRNA Release

The structure of the large ribosomal subunit was reported to be compact and monolithic.[32] Nevertheless, cryoelectron microscopy studies[79] showed that the features that are directly involved in ribosomal functions large subunit possess significant mobility. Similarly, the available crystal structures show that most of the functionally relevant features of the large subunit assume different conformations in assembled ribosomes[6] compared to the unbound state,[15,16] and may even become completely disordered (Figure 1), as is the case for the 2.4 Å structure of the large subunits from *Haloarcula marismortui,* H50S.[32]

The L1 stalk, which includes the rRNA helices 76–78 and the ribosomal protein L1, has a different conformation in isolation,[80] compared to the assembled ribosome.[6] Moreover, its orientation in the T70S ribosome[6] is radically different from that seen in the unbound D50S,[15] suggesting the mechanism whereby this arm facilitates the exit of the tRNA molecules. Thus, in the complex of T70S with three tRNA molecules, the L1 stalk interacts with the elbow of E-tRNA and seems to block the release of the E-site tRNA, whereas the location of the L1 stalk in D50S does not seem to block the presumed exit path of the E-site tRNA. Superposition of the structure of the internal part of the L1 stalk in D50S on that of the T70S ribosome allowed the definition of a pivot point for the possible movement of the L1 arm. Hence, it appears that the mobility of the L1 arm is utilized for facilitating the release of E-site tRNA (Figure 1).

An Intersubunit Bridge connecting the Decoding and the Peptidyl Transferase Sites

Intersubunit bridges form upon the association of the two ribosomal subunits, once the functionally active is created. They are the features connecting the two subunits within the assembled ribosome—namely, the linkers between the two ribosomal subunits. The correct assembly of the entire ribosome from its two subunits is the key, or one of the major keys, for proteins biosynthesis—hence these bridges must be positioned accurately and point at the exact direction. Each intersubunit bridge is formed from two parts—one of the small and one of the large subunits. We found that for most cases the parts associated with the intersubunit bridges that belong to the small subunit maintain a similar conformation in the bound and unbound states, whereas those originating from the large subunit are inherently flexible. Thus, they may appear disordered, as observed in the H50S structure,[32] or assume different conformations, hinting at the mechanism whereby the ribosome controls its subunit association.

Here we focus on bridge B2a, built of H69. In the 70S ribosome it stretches toward the small subunit, whereas in the unbound 50S it is located on the subunit surface. Figure 1 hints at a feasible sequence of events leading to its creation. Once the initiation complex, which includes the small subunit and a tRNA molecules at the P site, approaches the large subunit, the conformation of this complex dictates that it should be located in the space occupied by part of helix H69, and therefore pushed it towards the decoding center, creating the intersubunit bridge.

Analysis of the conformations of H69 in D50S and T70S indicates that the ribosome could benefit from the flexibility of H69 beyond its task in bridging the two subunits. Connecting between the peptidyl transferase center in the large subunit and the decoding region in the small one, H69 may be the right candidate to provide the machinery needed for the transmission of signals between the two centers. In addition, the proximity of H69 to both the A- and the P-site tRNAs,[2,6] suggest that besides acting as an intersubunit bridge, H69 may participate in translocation. The location of H69 may hint also at its contribution to a sophisticated signaling network over long distances, between the GTPase, the PTC center and between the PTC and the E-site tRNA release site.[15]

An Intergrated Ribosomal Machinery

A unified mechanism, which combines peptide-bond formation, translocation, and the entrance of nascent proteins into the exit tunnel, is described below. This mechanism is consistent with the suggestions that the main contribution of the ribosome in catalyzing peptidyl–transferase activity is the provision of a frame for precise positioning of the tRNA molecules.[2,15,16,40,81–87]

The counter proposal, deduced from the crystal structure of H50S in complex with a partially disordered tRNA-mimic and a material presumed to be a reaction intermediate, claimed that the ribosome participates actively in the enzymatic catalysis of the formation of the peptide bond.[88] Doubt concerning this proposal was raised based on biochemical and mutation data[45,86,89–91] and recent analysis of structures of additional complexes of the same particle, H50S, further substantiated these uncertainties. Thus, the PTC features that were originally suggested to catalyze peptide-bond formation were found in the recent complexes to point at a direction opposite to the peptide bond.[64,92]

We found that D50S crystals provide an excellent system for these experiments, since they were grown and maintained under conditions that are almost identical to those allowing for optimal biological activity.[15] We designed substrate analogs mimicking portions of the tRNA molecule that interacts with the large ribosomal subunit within the assembled ribosome—namely, the acceptor stem and the CCA 3′ end. The substrate analogs that were exploited ranged in size from puromycin derivatives to compounds mimicking the entire acceptor stem of tRNA, all of which posses a 3′-ACC–puromycin, corresponding to tRNA bases 73–76. The longest analog is a 35-nucleotide chain that mimics the entire acceptor stem of tRNA and its T-arm (called ASM). The shortest is a four-nucleotide chain representing the 3′ end of tRNA, called ACCP.[2]

Remote Interactions Dominate the Precise Positioning of the tRNA Molecules

Analysis of the interactions of ASM with the PTC of D50S indicated that ASM interacts with protein L16 and packs groove-to-backbone with the 23S RNA helix H69[2] (Figure 4). Originally, no protein was identified in the large ribosomal subunit from *H. marismortui* to be homologous of the eubacterial protein L16. However, structure similarity between D50S L16 and H50S L10e and their relative locations within the large ribosomal subunit revealed unambiguously that protein L10e has a prokaryotic, rather than eukaryotic, origin.[46] These comparisons also indicated the importance of L16 for protein biosynthesis, as

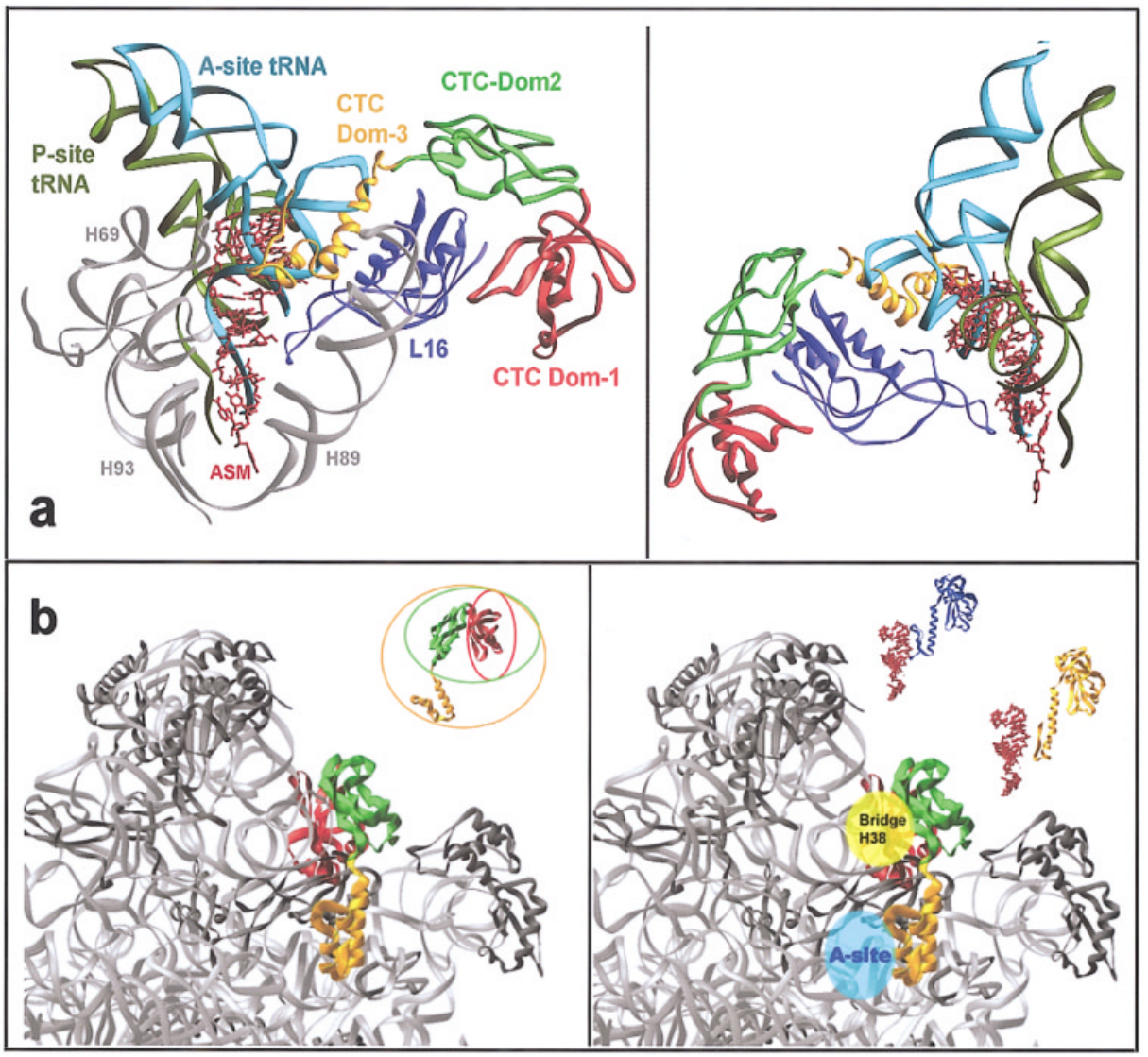

FIGURE 4 (a) Two approximately orthogonal views of the PTC and its environment in D50S, including a substrate analog (ASM) and the docked A- and P-site tRNAs. The remote interactions of ASM and the docked tRNA molecules with the walls of the PTC cavity are clearly observed. Highlighted are proteins L16 and helix H69. Also, the three domain of protein CTC, which undergoes substantial conformational changes upon ASM binding, although it does not interact with it, are shown. Domain-1, resembling protein L25 in red; domain-2, which together with domain 1 resemble protein TL5 in green; and domain-3, unique to *D. radiodurans,* in gold. (b) A zoom into the front side of D50S (the top-right and middle regions shown in FIGURE 1b). The proteins and the RNA backbones are shown in gray, except for protein CTC, which is colored according to the scheme in (a). On the right, approximate positions of the functional relevant features, namely: H38 which is the B1a intersubunit bridge (or the A-site finger) and the position of the acceptor stem of the A-site tRNA are overlaid (in yellow and cyan, respectively). Insert: the conformations of protein CTC in its native (blue) and in the complex with ASM (gold).

expected from a moiety assisting in the precise placement of A-site-tRNA.

The high-resolution crystal structures analyzed by us indicated that the precise positioning of the tRNA is dictated by its remote interactions. In the absence of such remote interactions, either because the substrate analogs are too short for these interactions, or due to disorder in the substrate interacting components, such as helix H69 in the H50S structure,[32] similar, albeit distinctly, different binding modes are formed (Figure

4). It is likely that the chemical nature of the analogs dictate the properties of their binding modes, neither of which is identical to that of ASM.[2] Analyses of the binding modes of the short or less well placed analogs showed that all are positioned with an orientation requiring conformational rearrangements in order to participate in peptide-bond formation.[64,88,92] These rearrangements are bound to consume time, thus rationalizing the relatively slow peptidyl-bond formation by short puromycin derivatives. In contrast to the not well-placed substrate analogs, ASM was found to be positioned correctly for peptide-bond formation,[2] confirming the suggestion that H69 and protein L16 are the key factors influencing the precise positioning of the tRNA within the PTC in an orientation that should lead to peptide-bond formation (Figure 4).

Flexible elements within the PTC

The conformational rearrangements of short or less well-placed longer substrate analogs may be assisted by the flexibility of the PTC. Variability in the PTC conformation, observed despite its high sequence conservation, could be correlated with phylogenetic variations,[60] as well as with the functional state of the ribosome. Thus, nucleotides showing different orientations in the T70S–tRNAs complex and in the structure of the liganded H50S were identified.[6] Furthermore, some of the variations of the PTC conformations that were observed between D50S and H50S crystal structures could be correlated to the significant distance from physiological conditions in the H50S environment.[32] This correlation is consistent with findings, accumulated over more than three decades, that variations of chemical conditions induce substantial conformational changes in the PTC of *E. coli* ribosomes.[45,93]

The diversity of the PTC binding modes observed in the different crystal forms indicates that the PTC tolerates various orientations of short puromycin derivatives. This suggests that the PTC inherent flexibility assists the conformational rearrangements required for substrate analogs bound in a nonproductive manner to participate in peptide-bond formation. The inherent flexibility of the PTC is demonstrated also by the action of the antibiotic sparsomycin, a potent ribosome-targeted inhibitor with a strong activity on all cell types, including Gram-positive bacteria and highly resistant archae.[47,56,94] We found that sparsomycin binds to the ribosome solely through stacking interactions with the highly conserved base A2602, consistent with crosslinks data[95] and rationalizing the difficulties of its localization.[38,56,62] Stacking interactions with A2602 were also observed in complexes of H50S,[64] albeit from the other side of the base. This finding is consistent with the fact that despite sparsomycin universality, ribosomes from various kingdoms display differences in binding affinities to it.[95]

A2602 is the PTC base that undergoes the largest conformational rearrangements observed so far as a consequence of substrate or inhibitor binding. It has a different orientation (Figure 3) in each of the known complexes of the large subunit.[2,3,18,64,88,92] This unique striking variability suggests that A2602 plays a dynamic role in motions within the PTC, and appears to function as a conformational switch, in concert with H69, which seems to assist the translocation event at the subunit interface.[2,15,16] Importantly, recent biochemical studies, showing the critical role of A2602,[96] support this suggestion.

A Sizable Symmetry-Related Region within the Asymmetric Ribosome

The ribosome is basically an asymmetric particle. Yet we detected an approximate twofold symmetry within the PTC of D50S, relating backbone fold and base conformation of two groups of about 90 nucleotides each[3] (Figure 5). This symmetry operation is consistent with the twofold symmetry observed between puromycin derivatives or tRNA 3′ termini in the active site of H50S[64,88,92] and T70S,[6] respectively, which shows that the tRNA 3′ ends are related by rotation while the tRNAs helical features are related by a shift.[6,67,97] The existence of twofold symmetry in all known structures of ribosomal large subunits indicates its universality.

The twofold-related region (Figure 5) consists of three semicircular shells, positioned between the two lateral protuberances of the large ribosomal subunit. The inner shell contains the PTC nucleotides that interact directly with the 3′-terminus and its amino acid of the bound tRNA or during its translocation.[2,3] It includes about half a dozen central loop nucleotides, the inner strands of H89 and H93 and the A and the P loops, which are the stem loops of helices H80 and H92. The second shell includes helices H80 and H92, the stems of the A and the P loops, as well as H74 and H90 that hold the P and the A loops, respectively. The outer shell includes the outer strands of H89 and H93 nucleotides that base pair with those belonging to the inner shell and the parts of H75 and H91 that are positioned close to the other components obeying the twofold symmetry.

The deviations from perfect twofold symmetry vary between nucleotides. Among the nucleotides composing the P site, four are located somewhat deeper in the PTC, compared to their mates at the A

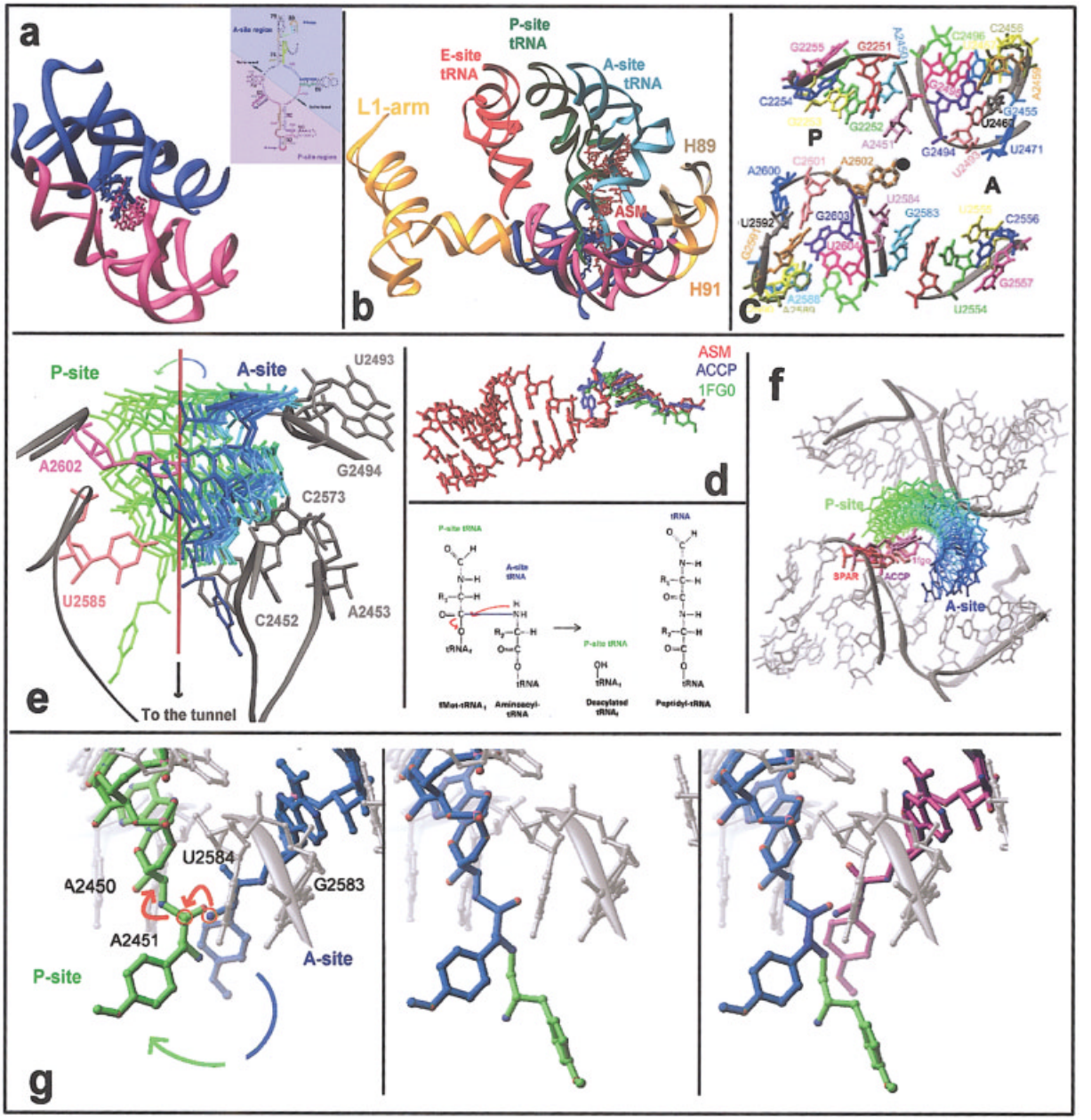

FIGURE 5 (a) The twofold related region, colored in purple and blue according to the two-dimensional diagram shown on the top right, together with the CCA ends of the A-site (purple) and the P-site (blue) tRNAs. (b) The twofold region, as shown in (a), together with the substrate analog, ASM (red), the P-site CCA end (blue), and the A-, P-, and E-site tRNAs (cyan, green, red). (c) A view into the active site, showing the inner shell of the symmetry-related region. (d) The differences between the binding modes of a well-placed substrate analog, ASM, compared to short compounds, ACCP and 1FG0.[88] Parts (e) and (f) show two views of the A- to P-passage motion of the correctly placed ASM analog, in which the rear-wall guidance and front nucleotides (A2602 and U2582) anchoring are readily observed. The blue-green arrow symbolizes the rotatory motion around the twofold axis (red). In (f) some the orientations of A2602 (see FIGURE 3h) are shown. (g) The proposed mechanism of peptide bond formation and A- to P translocation of the tRNA 3′ ends. The red arrows designate the path taken by the hydrogens, and the blue-green arrow the rotatory motion. Insert: the overall chemical reaction of formation of the peptide bond (blue). The red arrows designate the path taken by the hydrogens.

site. These are positioned at the entrance to the exit tunnel, and imply a modest spiral nature to the twofold axis.[2,3] An additional interesting deviation from the twofold symmetry is that observed for of G2250, which bulges out from the P loop and interacts with the flexible loop of protein L16, presumably stabilizing it in a conformation favorable for its interactions with the A-site tRNA. These interactions were found to provide the frame for correct positioning of the A-site tRNA (see above) and are hinting at an interplay between the P and the A sites within the PTC.

The Rotatory Motion from the A to the P Site

The presumed functional relevance of twofold symmetry indicates that the A- to P-site passage of the tRNA molecule involves two independent motions: a rotation of ~180° of the A-site tRNA 3′ end, performed in conjunction with peptide-bond formation and A- to P-site shift of the tRNA acceptor stem. Sovereign motions of tRNA structural features are also the basis of the hybrid-state translocation mechanism.[1,98] We observed that the P-O3′ bond the between the single-stranded 3′ end and the double-helical acceptor stem of ASM (corresponding to A-site tRNA 72–73) nearly overlaps with the twofold axis. We therefore defined the rotating moiety (RM) as the entire single-strand 3′end, namely tRNA 73–76 (ACCA).

In order to validate our proposed machinery we rotated, computationally, the RM of ASM[2,3] around the approximate twofold axis and derived a mimic of P-site 3′ end (Figure 5). This motion could be simulated with no space constraints or steric hindrance, and throughout the rotation no conformational adjustments were required. Moreover, this motion started and ended with both ASM and the derived P site interacting with the PTC RNA in a manner consistent with most of the available biochemical data.[99]

We found that the environment of the derived ASM–P-site 3′ end is similar to that of ASM, consistent with requirement to host both the A- and the P-site tRNA 3′ ends within the PTC while peptide bond is being formed. Furthermore, we observed that the A-site base pair shared by all known structures, between C75 of A-site tRNA and G2553,[100] can be formed in the symmetry-related region between G2251 and the C75 of the symmetry-derived 3′ end of ASM. Finally, the specific tasks of the P site in guiding the nascent chain into the tunnel seem to be performed by four nucleotides that are positioned lower in the PTC than their A-site mates, thus creating a configuration suitable for guarantying the entrance of the nascent protein into the exit tunnel.

While rotating, the RM interacts with several rear-wall bases, and slides along the backbone of other two (Figure 5). Two nucleotides of the PTC front-wall interact with RM. A2602, whose N1 atom sits on the twofold axis, is within contact distances to tRNA–A73 throughout the rotation. The second is U2585, which is located below A2602 close to the twofold axis and interacting with the rotated A76. We found that the space available for A2602 throughout the motion can accommodate its various conformations. Hence, it is conceivable that A2602 conformational variations are synchronized with the RM rotation. The conformation of the PTC front and rear walls in relation to the motion of the RM suggests that the rear wall forms a scaffold that guides the RM from the A to the P site. This guidance, together with the front-side double anchoring, provides the precise path for the rotating moiety. Most of the rear-wall nucleotides are highly conserved. One of the less conserved nucleotides is G2494. Its lower conservation is consistent with the utilization of its backbone phosphate, rather than it base, for guarding the RM motions. Its unique placement within the rear wall, intruding between the rotating C74 and C75, requires extra stabilization, which appears to be acquired by the adjacent A-minor motif of H39 and the nocanonical base pair with U2457.

The differences in the distances between the PTC rear and front walls from the RM could be correlated with their special tasks. The rear wall directs the motion of the RM, and thus had to be within interaction contact with it. The front wall, in comparison, contributes the two flexible anchoring nucleotides, A2585 and A2602, the bases of which seem to undergo conformational rearrangements together with the RM motion. Hence the backbone of the front wall is positioned in relatively large distance from the RM. Additional evidence for the rear-wall guidance was obtained from subsequent experiments, in which we allowed deviations from rigidity of the RM, consistent with the known flexibility of tRNA 3′ ends. In these exercises we found that the guidance of the rear-wall nucleotides together with the front anchoring restrict the possible motions of the RM nucleotides and limit their flexibility. Noteworthy is the finding that analysis of the 5.5 Å structure of T70S[6] indicates that base A73 of the tRNA is shifted together with tRNA acceptor stem, hence implying that the rotated moiety is C74–A76 rather than A73–A76. Our suggested motion holds for this case, but this rotating moiety will not be anchored to A2602, and the rotation will have to be simultaneous with the acceptor stem shift.

Peptide-Bond Formation: The Catalytic Action of the Ribosomes

The biological implication of the twofold rotation is the creation of a favorable geometry allowing peptide-bond formation with no further conformational rearrangements (Figure 5). Once properly positioned in the PTC, the guidance of the RM motion by the PTC nucleotides leads to orientation and distance suitable for a nucleophilic attack of the A-site primary amine on the P-site tRNA carbonyl–carbon. Such attack should readily occur at the pH of D50S crystals (around 7.8), which is also the pH optimized for functional activity of ribosomes from various sources, including *E. coli* and *H. marismortui.*[12,38,39,45,60,93,98] In the orientation resulting from the rotation, a tetrahedral oxyanion intermediate can be formed and the surrounding solvent may mediate the transfer of a hydrogen atom from the A-site tRNA α-amino group to the P-site tRNA leaving group. Release of the leaving group, namely the P-site tRNA, and the reorganization of the attacked electrophile from *sp3* to *sp2* hybridization will follow. In case stabilization of the oxyanion intermediate is required, it may be obtained by metal ions, such as hydrated Mg^{2+} ions, residing in the proximity of the oxyanion, or by a ribosomal moiety. If not, a spontaneous formation of the peptide bond is implied, as proposed over two decades ago.[81,83]

Apart from the GTPase hydrolysis, in comparison to the other steps of protein biosynthesis, the peptide-bond formation is considered to be a fast reaction.[101] This irreversible step appears to carry forward the entire protein biosynthesis process, including codon–anticodon recognition in the small subunit, the GTPase activation, and the A-site tRNA accommodation in the large subunit. We suggest that the degenerate frame resulting from the twofold symmetry has a crucial dynamic role. Once the incoming tRNA is positioned in the PTC in a favorable conformation, dictated by this frame, it has only to rotate into the second part of the frame. Saving reorganization time is crucial for faster reaction rates, enabling the conversion of the equilibrium of the chemical reaction to proceed toward peptide-bond formation.

We propose that the A- to P-site rotation is synchronized with peptide-bond formation, or triggered by it, and that by replacing the P-site tRNA–3′ end, the RM assists the release of the leaving group. Translocation of the acceptor stems of both tRNAs follows, freeing the space needed for binding of the next aminoacyl tRNA (Figure 5) so that the following synthetic cycle can take place. Our proposed mechanism for peptide-bond formation is consistent with results of footprinting experiments performed with 70S ribosome and tRNA molecules, showing that the A-tRNA acceptor stem moves spontaneously into the P site subsequent to peptide-bond formation.[87,98] The sole geometrical requirement for our proposed mechanism is that the 3′ end of the P-site tRNA in the initiation complex has a conformation related to that of the A site by an approximate twofold rotation.

Application of the rotatory motion to short A-site tRNA mimics,[2] as well as to acceptor stem mimics that are not well positioned due to the disorder of the ribosomal features that dictate the precise positioning of the A-site tRNA,[88] led to orientations that are less suitable for peptide-bond formation. Although it is conceivable that substrate analogs that do not possess optimal geometry can form a single peptide bond, after rearrangements, it is clear that unless the creation of the bond is accompanied by A- to P-site passage, no further protein biosynthesis can take place. The fragment assay performed within H50S crystals provide a suitable example. In this assay an A-site bound product, CCA–puromycin–phenylalanine–caproic-acid–biotin, was formed from two puromycin derivatives. This product was not passed to the P site[92] either because its initial binding geometry was not suitable for the specific RM rear-wall interactions, or due to the low affinity of puromycin products to the P site.[64,92] Additional biological implications of the suggested motion are the efficient replacement of the P-site 3′ end by the RM, and the assistance given to the nascent chain to migrate into the exit tunnel by the P-site nucleotides that interact with the RM. These are located at the bottom of the PTC in a configuration ensuring that the translocation motion into the P site will deliver the newly born polypeptide into the tunnel entrance.

To conclude: we found that correct positioning of the A-site tRNA stimulates the flip of its 3′ end into the position of the 3′ end of the P-site tRNA, and we suggest that this rotation occurs in concert with peptide-bond formation. The results of this motion are a peptidyl chain that points into the entrance to the protein exit tunnel and a translocation of the deacylated P-site tRNA into the E site. This simple mechanism is consistent with earlier proposals that the main enzymatic contribution of the ribosome in protein biosynthesis is the provision of a frame for accurate positioning of the tRNA molecules, consistent with results of previous biochemical experiments.[81,83,87,98] In the absence of precise positioning, the inherent flexibility of the peptidyl transferase center allows various binding modes, all requiring conformational rearrangements for participating in peptide-bond formation.

Transmission of Information Between the Two Ribosomal Protuberances

About a dozen nucleotides of the symmetry-related region create the environments of the 3′ end termini of the A- and the P-site tRNA molecules. The remaining nucleotides of the twofold symmetry-related region extends between the two lateral protuberances of the large ribosomal subunit. It connects the stems of the L1 and the L7/L12 stalks (consisting of H76–H78 and protein L1, and H43–H44, the sarcin–ricin site, the loop of H95, and proteins L10, L11, and L12, respectively). H76–H78 are directly connected to H75, and, from the opposite side, helix H91 reaches the sarcin–ricin loop and the part of helix H89 that does not obey the twofold symmetry, interacts indirectly with H43–H44. Both features are involved in functional activities of the ribosome. L7/L12 stalk, which contains also protein L11 and the sarcin–ricin loop, is involved in the contacts with the translocational factors, in factor-dependent GTPase,[102] and in elongation factor activity,[103] thus playing a major role in the entrance of the aa-tRNA into the functioning ribosome. The L1 stalk, from the other hand, is facilitating the release of the E-site tRNA molecules (see above).

Analysis of the structure of the symmetry-related region suggests that each of its three shells has a specific task.[3] As mentioned above, the inner shell appears to provide similar environments within the PTC for the A- and the P-site tRNA, consistent with requirement to host both termini while peptide bond is being formed (Figure 5). H74 and H90, of the second shell, are the long helical features that connect between the sequence-distant P and the A loops and the inner shell, via H80 and H92, respectively, thus maintaining the symmetrical requirements of the PTC. Therefore increasing the stability of the PTC core structure may be the task of the second shell of the symmetry-related region.[3]

Transmission of signals between ribosomal features that are involved in the entire process of protein biosynthesis may be associated with the symmetry-related region. As mentioned above, features radiating from the outer shell of the symmetry-related region interact with the L1 and the L7/L12 stalks. It is, therefore, conceivable that the outer shell of the symmetry-related region plays a role in the transmission of signals between the ribosomal features facilitating the two ends of the biosynthetic process: in the entry of the amino acylated tRNA that is about to participate in peptide-bond formation, and in the release of the free E-site tRNA, after the formation of the peptide bond.

A Ribosomal Protein Regulating tRNA Binding

CTC is a ribosomal protein that undergoes conformational changes upon ASM binding to D50S, although it does not interact directly with the bound ASM. This protein, named after a general shock protein, is one of the D50S novel features. It replaces the *E. coli* protein L25 and its *T. thermophilus* homologue, TL5. Among the known members of the CTC protein family, the *D. radiodurans* CTC is the longest. It contains three domains (Figure 4). The N-terminal and middle domains of CTC (N-CTC and M-CTC, respectively), fold with a topology close to that of protein TL5,[104] and the structure of CTC N-terminal domain is similar to that of protein L25 from *E. coli.*[105] In D50S, N-CTC is located on the solvent side and interacts with the 5S RNA, and we suggest that this is the position of L25 in *E. coli* and of the N-terminal domain of TL5 in *T. thermophilus* ribosomes. Similarly, we presume that the location of M-CTC represents that of C-TL5 in *T. thermophilus* ribosome.

Protein CTC fills the space between the 5S and the L11 arm, and wraps a large part of helix H38 that forms the B1a intersubunit bridge, called also the A-site finger.[6] This bridge is highly flexible, and thus can readily become disordered, as seen in the structure of H50S, similar to other intersubunit bridges, namely B1b and B2a.[32]Based on the position of N-CTC on the backside of the central protuberance near B1b intersubunit bridge, we suggest that N-CTC protects this functionally important region from uncontrolled movements or interactions. Further protection appears to be provided by M-CTC (or the C-terminal domain of TL5) since they wrap this region, thus capable of preventing sliding of the intersubunit B1a bridge to wrong directions, which is likely to occur at the elevated temperatures required for efficient functioning of *T. thermophilus* ribosome. A similar protection mechanism was detected in the *T. thermophilus* small ribosomal subunit. Protein S17 from this source was associated with thermal stability, since mutants lacking it display temperature sensitivity,[106] and only in thermophilic bacteria (*T. Thermus aquaticus* and *Thermotoga maritima*) does S17 possess a long C-terminal tail, consisting of over 22 amino acids. Protein S17 is located near the platform of the small subunit,[28,29] known to participate in the motions that assist translocation. The S17 long α-helical tail curls within a narrow groove that separates the platform from the body, following the contour of the platform, thus situated in a position that can act as a physical stopper that blocks uncontrolled sliding of the platform that may occur at elevated temperature.

The C-terminal domain of CTC is placed at the rim of the intersubunit interface, reaching the location of the acceptor stem of the docked A-site tRNA. It interacts with the flexible B1a bridge and should restrict the space available for the A-site tRNA. As the C-terminal domain of CTC is connected to the middle domain by a linker that seems to be highly flexible (Figure 4), we suggested that C-CTC serves as an A-site binding regulator,[15,16] as confirmed by ASM binding. It seems that the mechanism of regulating A-site tRNA binding is based on space exclusion, with the slender connection between M-CTC and C-CTC allowing for the swinging of C-CTC from its native location, where it might have collided with the acceptor stem of A-site tRNA, to the location that it adopts for facilitating ASM binding. It seems, therefore, that each of the three domains of CTC has a specific function, hinting at a possible connection between the three domains of this protein (N-, M-, and C-CTC) and lives under mild, thermophilic, and stressful conditions, respectively. Thus, the interactions of CTC with the solvent side of the large subunit central protuberance, its ability to manipulate the A-site tRNA binding and to enhance the stability of the B1b intersubunit bridge, may be connected to the mechanisms that *D. radiodurans* developed for survival.

POSTPEPTIDE-BOND FORMATION—GATING AND DISCRIMINATION

Once produced, the nascent proteins emerge out of ribosomes through the tunnel adjacent to the PTC. This tunnel was recently shown to undergo alterations associated with antibiotic-resistant mutations,[66] to posses discriminating properties, and to participate in regulating intracellular cotranslational processes.[107–113] Striking examples are the *secM* (secretion monitor) protein[110,112] and the nascent leader peptide of *E. coli* tryptophanase (tnaC) operon. The *SecM* protein is produced in conjunction with a protein-export system, which recognizes an export signal located at the protein N-terminus.[112] This protein includes the sequence motif that in the absence of the protein-export system causes arrest during translation. This motif was shown to induce elongation arrest in *E. coli* while SecM protein is being synthesized and to hinder translation elongation when present in the unrelated sequence of LacZ α protein,[112] indicating that the elongation arrest is independent of the sequence context. Within this sequence, Pro, Trp, and Ile were identified to be the main features that trigger the arrest.

Mutations in the 23S ribosomal RNA or in ribosomal protein L22,[112] a constituent of the tunnel wall[15,88] bypass the elongation arrest. Protein L22 consists of a single globular domain and a highly conserved β-hairpin that has a unique twisted conformation. This β-hairpin maintains its length in all species, whereas insertions as well as deletions exist in other regions of L22. Within the ribosome, protein L22 is positioned with its globular domain on the surface of the large subunit, whereas its β-hairpin lines the protein exit tunnel wall and extends approximately 30 Å away from the protein core.[15,88] The overall conformation of L22 in the ribosome is similar to that seen in its crystal structure,[65] except for a small difference in the inclination of the tip of the β-hairpin. As mentioned above this tip is rather flexible, and can flip across the tunnel and interact with its both sides.[3,20] We suggest that a similar swing of the tip of the β-hairpin of protein L22 is involved in the regulatory role assigned to the tunnel. It appears, therefore, that protein L22 is a main player in the tunnel gating, that its double hook acts as a conformational switch, providing the molecular tool for the discriminative properties of the ribosome tunnel.

The sequence motif shown to induce elongation arrest in *E. coli* while the SecM protein is being formed, FXXXXWIXXXXGIRAGP, includes three residues, Pro, Trp, and Ile, adjacent to the Trp, that were found to be the main features that trigger the arrest,[112] A similar sequence that causes arrest was identified in the leader peptide of *E. coli* tryptophanase (tnaC) operon.[113] Hence, it seems that the combination of the conformational requirements for both Trp and Pro causes the elongation arrest in the SecM. We verified that once a proline has reached the tunnel entrance, i.e., it has been incorporated into the nascent chain, the crucial Trp residue reaches the tip of L22 β-hairpin, by modeling the nascent chain within the exit tunnel. Thus, the rigidity of Pro restricts the conformational space of the entire sequence, minimizing the motions required for progression of the nascent chain within the tunnel. These restrictions should force the Trp to trigger an alteration in the L22 β-hairpin, in a manner similar to the action of TAO. The swinging of the L22 tip frees space for the bulky side chains, and at the same time jams the tunnel for the progression of bulky nascent chains.

Elongation arrest of SeqM sequence was found to ease in the presence of active export of SecM.[112] We suggest that the cellular signaling for alleviating the arrest is being transmitted from the environment into the ribosomes through L22 β-strand extension of the hairpin, which extends all the way to the tunnel opening.[15,32] The nascent chain itself may also play a role

in the suppression of the elongation arrest, since when the ribosome is stalled, the export signaling sequence of SecM has already emerged out of the exit tunnel. The common sequence dependence of the elongation arrest, the existence of arrest-suppression mutations that should affect the conformation of the highly conserved L22 β-hairpin, indicate the universality of the tunnel gating abilities.

CONCLUSIONS

Ribosomal crystallography, initiated two decades ago, yielded exciting structural and clinical information. Apart from the structures themselves, which provide immense structural information, insights into the mechanisms of decoding, peptide-bond formation and translocation are emerging. Thus, we showed that remote directionality is the main factor for correct positioning of the tRNA in the PTC, and that precisely positioned tRNA analogs allow a spiral rotation of the 3′ end of the A-tRNA around a symmetry axis identified by us in all known structures of the large subunit, which result in an orientation suitable for peptide-bond formation and for the guidance of the nascent chain into the exit tunnel. Based on the conformation of the PTC rear wall, we conclude that it forms a scaffold guiding this rotation and the PTC front-side nucleotides anchor the rotating moiety. Our results also show that the exit tunnel possesses intrinsic conformational mobility, and that a protein component of the tunnel walls can swing across it, allowing for discriminative gating of the nascent protein.

The identification of a twofold symmetry in all known structures of the large subunit, the high conservation of most nucleotides belonging to the inner symmetry-related region, the ensured entrance of nascent proteins into the tunnel, the possible mediation of signal transmissions between the incoming and the leaving tRNA molecules by the symmetry-related region, as well as the resulting mutual orientation of A- and P-site tRNAs suitable for peptide-bond formation, are consistent with the universality of our proposed mechanism.

Besides better understanding of the process of protein biosynthesis, our studies were found suitable to serve as pathogen models capable of supplying information on antibiotics binding at the molecular detail. The elucidation of the inhibitory mechanisms of the ribosomal antibiotics should pave the way for structure-based drug design of novel antimicrobial agents with minimized resistance abilities and maximal binding properties.

Thanks are due to J. M. Lehn and M. Lahav for critical discussions, M. Pope for supplying us with tungsten clusters, and to all the member of the ribosomal-crystallography groups at the Weizmann Institute and the Max–Planck Society for contributing to different stages of these studies. These studies could not be performed without the cooperation and assistance of the staff of station ID19 of the SBC at APS/ANL and IDAY at ESRF/EMBL. The Max–Planck Society, the U.S. National Institute of Health (GM34360), the German Ministry for Science and Technology (BMBF Grant 05-641EA), and the Kimmelman Center for Macromolecular Assembly at the Weizmann Institute provided support. AY holds the Helen and Martin Kimmel Professorial Chair.

REFERENCES

1. Noller, H. F.; Yusupov, M. M.; Yusupova, G. Z.; Baucom, A.; Cate, J. H. FEBS Lett 2002, 514, 11–16.
2. Bashan, A.; Agmon, I.; Zarivach, R.; Schluenzen, F.; Harms, J.; Berisio, R.; Bartels, H.; Franceschi, F.; Auerbach, T.; Hansen, H. A. S.; Kossoy, E.; Kessler, M.; Yonath, A. Mol Cell 2003, 11, 91–102.
3. Agmon, I.; Auerbach, T.; Baram, D.; Bartels, H.; Bashan, A.; Berisio, R.; Fucini, P.; Hansen, H. A. S.; Harms, J.; Kessler, M.; Schluenzen, F.; Yonath, A.; Zarivach, R. Eur J Biochem, 2003, 270, 2543–2556.
4. Yonath, A.; Muessig, J.; Tesche, B.; Lorenz, S.; Erdmann, V. A.; Wittmann, H. G. Biochem Int 1980, 1, 315–428.
5. Hansen, H. A.; Volkmann, N.; Piefke, J.; Glotz, C.; Weinstein, S.; Makowski, I.; Meyer, S.; Wittmann, H. G.; Yonath, A. Biochim Biophys Acta 1990, 1050, 1–7.
6. Yusupov, M. M.; Yusupova, G. Z.; Baucom, A.; Lieberman, K.; Earnest, T. N.; Cate, J. H.; Noller, H. F. Science 2001, 292, 883–896.
7. Yonath, A.; Bartunik, H. D.; Bartels, K. S.; Wittmann, H. G. J Mol Biol 1984, 177, 201–206.
8. Muessig, J.; Makowski, I.; von Bohlen, K.; Hansen, H.; Bartels, K. S.; Wittmann, H. G.; Yonath, A. J Mol Biol 1989, 205, 619–621.
9. Volkmann, N.; Hottentrager, S.; Hansen, H. A.; Zaytzev-Bashan, A.; Sharon, R.; Berkovitch-Yellin, Z.; Yonath, A.; Wittmann, H. G. J Mol Biol 1990, 216, 239–241.
10. Yonath, A.; Glotz, C.; Gewitz, H. S.; Bartels, K. S.; von Bohlen, K.; Makowski, I.; Wittmann, H. G. J Mol Biol 1988, 203, 831–834.
11. Trakhanov, S. D.; Yusupov, M. M.; Agalarov, S. C.; Garber, M. B.; Ryazantsev, S. N.; Tischenko, S. V.; Shirokov, V. A. FEBS Lett 1987, 220, 319–322.
12. Shevack, A.; Gewitz, H. S.; Hennemann, B.; Yonath, A.; Wittmann, H. G. FEBS Lett 1985, 184, 68–71.

13. Makowski, I.; Frolow, F.; Saper, M. A.; Shoham, M.; Wittmann, H. G.; Yonath, A. J Mol Biol 1987, 193, 819–822.
14. von Bohlen, K.; Makowski, I.; Hansen, H. A.; Bartels, H.; Berkovitch-Yellin, Z.; Zaytzev-Bashan, A.; Meyer, S.; Paulke, C.; Franceschi, F.; Yonath, A. J Mol Biol 1991, 222, 11–15.
15. Harms, J.; Schluenzen, F.; Zarivach, R.; Bashan, A.; Gat, S.; Agmon, I.; Bartels, H.; Franceschi, F.; Yonath, A. Cell 2001, 107, 679–688.
16. Yonath, A. Annu Rev Biophys Biomol Struct 2002, 31, 257–273.
17. Zarivach, R.; Bashan, A.; Schluenzen, F.; Harms, J.; Pioletti, M.; Franceschi, F.; Yonath, A. Curr Protein Peptide Sci 2002, 3, 55–65.
18. Schluenzen, F.; Zarivach, R.; Harms, J.; Bashan, A.; Tocilj, A.; Albrecht, R.; Yonath, A.; Franceschi, F. Nature 2001, 413, 814–821.
19. Schluenzen, F.; Harms, J.; Franceschi, F.; Hansen, H. A. S.; Bartels, H.; Zarivach, R.; Yonath, A. Structure 2003, 11, 329–338.
20. Berisio, R.; Schluenzen, F.; Harms, J.; Bashan, A.; Yonath, A. Nat Struc Biol 2003, 10, 266–290.
21. White, O.; Eisen, J. A.; Heidelberg, J. F.; Hickey, E. K.; Peterson, J. D.; Dodson, R. J.; Haft, D. H.; Gwinn, M. L.; Nelson, W. C.; Richardson, D. L.; Moffat, K. S.; Qin, H.; Jiang, L.; Pamphile, W.; Crosby, M.; Shen, M.; Vamathevan, J. J.; Lam, P.; McDonald, L.; Utterback, T.; Zalewski, C.; Makarova, K. S.; Aravind, L.; Daly, M. J.; Fraser, C. M.; et al. Science 1999, 286, 1571–1577.
22. Levin-Zaidman, S.; Englander, J.; Shimoni, E.; Sharma, A. K.; Minton, K. W.; Minsky, A. Science 2003, 299, 254–256.
23. Hope, H.; Frolow, F.; von Bohlen, K.; Makowski, I.; Kratky, C.; Halfon, Y.; Danz, H.; Webster, P.; Bartels, K. S.; Wittmann, H. G.; et al. Acta Crystallogr B 1989, 45, 190–199.
24. Yonath, A.; Leonard, K. R.; Weinstein, S.; Wittmann, H. G. Cold Spring Harb Symp Quant Biol 1987, 52, 729–741.
25. Huang, H.; Chopra, R.; Verdine, G. L.; Harrison, S. C. Science 1998, 282, 1669–1675.
26. Luger, K.; Mader, A. W.; Richmond, R. K.; Sargent, D. F.; Richmond, T. J. Nature 1997, 389, 251–260.
27. Pioletti, M.; Schluenzen, F.; Harms, J.; Zarivach, R.; Gluhmann, M.; Avila, H.; Bashan, A.; Bartels, H.; Auerbach, T.; Jacobi, C.; Hartsch, T.; Yonath, A.; Franceschi, F. EMBO J 2001, 20, 1829–39.
28. Schluenzen, F.; Tocilj, A.; Zarivach, R.; Harms, J.; Gluehmann, M.; Janell, D.; Bashan, A.; Bartels, H.; Agmon, I.; Franceschi, F.; Yonath, A. Cell 2000, 102, 615–623.
29. Wimberly, B. T.; Brodersen, D. E.; Clemons, W. M., Jr.; Morgan–Warren, R. J.; Carter, A. P.; Vonrhein, C.; Hartsch, T.; Ramakrishnan, V. Nature 2000, 407, 327–339.
30. Stoffler, G.; Stoffler-Meilicke, M. Annu Rev Biophys Bioeng 1984, 13, 303–330.
31. Lake, J. A. Annu Rev Biochem 1985, 54, 507–530.
32. Ban, N.; Nissen, P.; Hansen, J.; Moore, P. B.; Steitz, T. A. Science 2000, 289, 905–920.
33. Mueller, F.; Sommer, I.; Baranov, P.; Matadeen, R.; Stoldt, M.; Wohnert, J.; Gorlach, M.; van Heel, M.; Brimacombe, R. J Mol Biol 2000, 298, 35–59.
34. Penczek, P.; Ban, N.; Grassucci, R. A.; Agrawal, R. K.; Frank, J. J Struct Biol 1999, 128, 44–50.
35. Ginzburg, M.; Sachs, L.; Ginzburg, B. Z. J Gen Physiol 1970, 55, 187–207.
36. Cundliffe, E. In The Ribosome: Structure, Function and Evolution; Hill, W. E., Dahlberg, A. E., Garrett, R. A., Moore, P. B., Schlessinger, D., Warner, J. R., Eds.; ASM: Washington, DC, 1990; pp 479–490.
37. Garrett, R. A.; Rodriguez-Fonseca, C. In Ribosomal RNA: Structure, Evolution, Processing & Function; Zimmermann, R. A., Dahlberg, A. E., Eds.; CRC Press: Boca Raton, FL, 1995; pp 327–355.
38. Moazed, D.; Noller, H. F. Proc Natl Acad Sci USA 1991, 88, 3725–3728.
39. Noller, H. F.; Hoffarth, V.; Zimniak, L. Science 1992, 256, 1416–1419.
40. Samaha, R. R.; Green, R.; Noller, H. F. Nature 1995, 377, 309–314.
41. Milligan, R. A.; Unwin, P. N. Nature 1986, 319, 693–695.
42. Yonath, A.; Leonard, K. R.; Wittmann, H. G. Science 1987, 236, 813–816.
43. Malkin, L. I.; Rich, A. J Mol Biol 1967, 26, 329–346.
44. Sabatini, D. D.; Blobel, G. J Cell Biol 1970, 45, 146–157.
45. Bayfield, M. A.; Dahlberg, A. E.; Schulmeister, U.; Dorner, S.; Barta, A. Proc Natl Acad Sci USA 2001, 98, 10096–10101.
46. Harms, J.; Schluenzen, F.; Zarivach, R.; Bashan, A.; Bartels, H.; Agmon, I.; Yonath, A. FEBS Lett 2002, 525, 176.
47. Cundliffe, E. Antibiotic Inhibitors of Ribosome Function; Wiley: London, New York, Sydney, Toronto, 1981.
48. Weisblum, B. Antimicrob Agents Chemother 1995, 39, 577–585.
49. Spahn, C. M.; Prescott, C. D. J Mol Med 1996, 74, 423–439.
50. Douthwaite, S.; Hansen, L. H.; Mauvais, P. Mol Microbiol 2000, 36, 183–193.
51. Auerbach, T.; Bashan, A.; Harms, J.; Schluenzen, F.; Zarivach, R.; Bartels, H.; Agmon, I.; Kessler, M.; Pioletti, M.; Franceschi, F.; Yonath, A. Curr Drug Targets—Infectious Disorders 2002, 2, 169–186.
52. Brodersen, D. E.; Clemons, W. M., Jr.; Carter, A. P.; Morgan-Warren, R. J.; Wimberly, B. T.; Ramakrishnan, V. Cell 2000, 103, 1143–1154.

53. Carter, A. P.; Clemons, W. M.; Brodersen, D. E.; Morgan-Warren, R. J.; Wimberly, B. T.; Ramakrishnan, V. Nature 2000, 407, 340–348.
54. Hansen, J. L.; Ippolito, J. A.; Ban, N.; Nissen, P.; Moore, P. B.; Steitz, T. A. Mol Cell 2002, 10, 117–128.
55. Traut, R. R.; Monro, R. E. J Mol Biol 1964, 10, 63–72.
56. Vazquez, D. Mol Biol Biochem Biophys 1979, 30, 1–312.
57. Porse, B. T.; Garrett, R. A. J Mol Biol 1995, 249, 1–10.
58. Kirillov, S.; Porse, B. T.; Vester, B.; Woolley, P.; Garrett, R. A. FEBS Lett 1997, 406, 223–233.
59. Rodriguez-Fonseca, C.; Phan, H.; Long, K. S.; Porse, B. T.; Kirillov, S. V.; Amils, R.; Garrett, R. A. RNA 2000, 6, 744–754.
60. Porse, B. T.; Kirillov, S. V.; Awayez, M. J.; Ottenheijm, H. C.; Garrett, R. A. Proc Natl Acad Sci USA 1999, 96, 9003–9008.
61. Lazaro, E.; Rodriguez-Fonseca, C.; Porse, B.; Urena, D.; Garrett, R. A.; Ballesta, J. P. J Mol Biol 1996, 261, 231–238.
62. Tan, G. T.; DeBlasio, A.; Mankin, A. S. J Mol Biol 1996, 261, 222–230.
63. Chepkwony, H. K.; Roets, E.; Hoogmartens, J. J Chromatogr A 2001, 914, 53–58.
64. Hansen, J. L.; Schmeing, T. M.; Moore, P. B.; Steitz, T. A. Proc Natl Acad Sci USA 2002, 16, 16.
65. Unge, J.; Berg, A.; Al-Kharadaghi, S.; Nikulin, A.; Nikonov, S.; Davydova, N.; Nevskaya, N.; Garber, M.; Liljas, A. Structure 1998, 6, 1577–1586.
66. Gabashvili, I. S.; Gregory, S. T.; Valle, M.; Grassucci, R.; Worbs, M.; Wahl, M. C.; Dahlberg, A. E.; Frank, J. Mol Cell 2001, 8, 181–188.
67. Stark, H.; Orlova, E. V.; Rinke-Appel, J.; Junke, N.; Mueller, F.; Rodnina, M.; Wintermeyer, W.; Brimacombe, R.; van Heel, M. Cell 1997, 88, 19–28.
68. Evers, U.; Franceschi, F.; Boddeker, N.; Yonath, A. Biophys Chem 1994, 50, 3–16.
69. Berkovitch-Yellin, Z.; Bennett, W. S.; Yonath, A. Crit Rev Biochem Mol Biol 1992, 27, 403–444.
70. Zamir, A.; Miskin, R.; Elson, D. J Mol Biol 1971, 60, 347–364.
71. Tocilj, A.; Schlunzen, F.; Janell, D.; Gluhmann, M.; Hansen, H. A.; Harms, J.; Bashan, A.; Bartels, H.; Agmon, I.; Franceschi, F.; Yonath, A. Proc Natl Acad Sci USA 1999, 96, 14252–14257.
72. Schlunzen, F.; Bashan, A.; Franceschi, F.; Yonath, A. Structure Fold Des 1999, 7, 931–941.
73. Kozak, M.; Shatkin, A. J. J Biol Chem 1978, 253, 6568–6577.
74. Kurylo-Borowska, Z. Biochim Biophys Acta 1975, 399, 31–41.
75. Fresno, M.; Carrasco, L.; Vazquez, D. Eur J Biochem 1976, 68, 355–364.
76. Moazed, D.; Samaha, R. R.; Gualerzi, C.; Noller, H. F. J Mol Biol 1995, 248, 207–210.
77. Mankin, A. S. J Mol Biol 1997, 274, 8–15.
78. Woodcock, J.; Moazed, D.; Cannon, M.; Davies, J.; Noller, H. F. EMBO J 1991, 10, 3099–3103.
79. Frank, J.; Agrawal, R. K. Nature 2000, 406, 318–322.
80. Nikulin, A.; Eliseikina, I.; Tishchenko, S.; Nevskaya, N.; Davydova, N.; Platonova, O.; Piendl, W.; Selmer, M.; Liljas, A.; Drygin, D.; Zimmermann, R.; Garber, M.; Nikonov, S. Nat Struct Biol 2003, 6, 6.
81. Cooperman, B. S. Adv Exp Med Biol 1977, 595–609.
82. Krayevsky, A. A.; Kukhanova, M. K. Prog Nucleic Acid Res Mol Biol 1979, 23, 1–51.
83. Nierhaus, K. H.; Schulze, H.; Cooperman, B. S. Biochem Int 1980, 1, 185–192.
84. Green, R.; Noller, H. F. Annu Rev Biochem 1997, 66, 679–716.
85. Pape, T.; Wintermeyer, W.; Rodnina, M. EMBO J 1999, 18, 3800–3807.
86. Polacek, N.; Gaynor, M.; Yassin, A.; Mankin, A. S. Nature 2001, 411, 498–501.
87. Wilson, K. S.; Noller, H. F. Cell 1998, 92, 337–349.
88. Nissen, P.; Hansen, J.; Ban, N.; Moore, P. B.; Steitz, T. A. Science 2000, 289, 920–930.
89. Barta, A.; Dorner, S.; Polacek, N. Science 2001, 291, 203.
90. Thompson, J.; Kim, D. F.; O'Connor, M.; Lieberman, K. R.; Bayfield, M. A.; Gregory, S. T.; Green, R.; Noller, H. F.; Dahlberg, A. E. Proc Natl Acad Sci USA 2001, 98, 9002–9007.
91. Parnell, K. M.; Seila, A. C.; Strobel, S. A. Proc Natl Acad Sci USA 2002, 16, 16.
92. Schmeing, T. M.; Seila, A. C.; Hansen, J. L.; Freeborn, B.; Soukup, J. K.; Scaringe, S. A.; Strobel, S. A.; Moore, P. B.; Steitz, T. A. Nat Struct Biol 2002, 9, 225–230.
93. Miskin, R.; Zamir, A.; Elson, D. Biochem Biophys Res Commun 1968, 33, 551–557.
94. Goldberg, I. H.; Mitsugi, K. Biochem Biophys Res Commun 1966, 23, 453–459.
95. Lazaro, E.; van den Broek, L. A.; San Felix, A.; Ottenheijm, H. C.; Ballesta, J. P. Biochemistry 1991, 30, 9642–9648.
96. Polocek, N.; Gomez, M. J.; Ito, K.; Xiong, L.; Nakamura, Y.; Mankin, A. Mol Cell 2003, 11, 103–112.
97. Agrawal, R. K.; Heagle, A. B.; Penczek, P.; Grassucci, R. A.; Frank, J. Nat Struct Biol 1999, 6, 643–647.
98. Moazed, D.; Noller, H. F. Nature 1989, 342, 142–148.
99. Green, R.; Noller, H. F. Biochemistry 1999, 38, 1772–1779.
100. Kim, D. F.; Green, R. Mol Cell 1999, 4, 859–864.
101. Rodnina, M. V.; Wintermeyer, W. Trends Biochem Sci 2001, 26, 124–130.
102. Chandra Sanyal, S.; Liljas, A. Curr Opin Struct Biol 2000, 10, 633–636.
103. Cundliffe, E.; Dixon, P.; Stark, M.; Stoffler, G.; Ehrlich, R.; Stoffler-Meilicke, M.; Cannon, M. J Mol Biol 1979, 132, 235–252.

104. Fedorov, R.; Meshcheryakov, V.; Gongadze, G.; Fomenkova, N.; Nevskaya, N.; Selmer, M.; Laurberg, M.; Kristensen, O.; Al-Karadaghi, S.; Liljas, A.; Garber, M.; Nikonov, S. Acta Crystallogr D Biol Crystallogr 2001, 57, 968–976.
105. Lu, M.; Steitz, T. A. Proc Natl Acad Sci USA 2000, 97, 2023–2028.
106. Simitsopoulou, M.; Avila, H.; Franceschi, F. Eur J Biochem 1999, 266, 524–532.
107. Liao, S.; Lin, J.; Do, H.; Johnson, A. E. Cell 1997, 90, 31–41.
108. Stroud, R. M.; Walter, P. Curr Opin Struct Biol 1999, 9, 754–759.
109. Morris, D. R.; Geballe, A. P. Mol Cell Biol 2000, 20, 8635–8642.
110. Sarker, S.; Rudd, K. E.; Oliver, D. J Bacteriol 2000, 182, 5592–5595.
111. Tenson, T.; Ehrenberg, M. Cell 2002, 108, 591–594.
112. Nakatogawa, H.; Ito, K. Cell 2002, 108, 629–636.
113. Gong, F.; Yanofsky, C. Science 2002, 297, 1864–1867.